

Original Article  
Biomedical Engineering



OPEN ACCESS

Received: Apr 7, 2020

Accepted: Aug 20, 2020

Address for Correspondence:

Se Heang Oh, PhD

Department of Nanobiomedical Science & BK21 PLUS NBM Global Research Center for Regenerative Medicine, Dankook University, 119 Dandae-ro, Dongnam-gu, Cheonan 31116, Republic of Korea.

E-mail: seheangoh@dankook.ac.kr

Tae Gyun Kwon, MD, PhD

Department of Urology, Kyungpook National University Chilgok Hospital, 807 Hoguk-ro, Buk-gu, Daegu 41404, Republic of Korea.

E-mail: tgkwon@knu.ac.kr

\*Ho Yong Kim and So Young Chun contributed equally to this work.

© 2020 The Korean Academy of Medical Sciences.

This is an Open Access article distributed under the terms of the Creative Commons Attribution Non-Commercial License (<https://creativecommons.org/licenses/by-nc/4.0/>) which permits unrestricted non-commercial use, distribution, and reproduction in any medium, provided the original work is properly cited.

ORCID iDs

Ho Yong Kim

<https://orcid.org/0000-0001-8187-5666>

So Young Chun

<https://orcid.org/0000-0003-4500-4956>

Eun Hye Lee

<https://orcid.org/0000-0001-5507-2632>

Bomi Kim

<https://orcid.org/0000-0002-0878-4765>

# Bladder Regeneration Using a Polycaprolactone Scaffold with a Gradient Structure and Growth Factors in a Partially Cystectomized Rat Model

Ho Yong Kim <sup>1\*</sup>, So Young Chun <sup>2\*</sup>, Eun Hye Lee <sup>3</sup>, Bomi Kim <sup>2</sup>,  
Yun-Sok Ha <sup>4,5</sup>, Jae-Wook Chung <sup>5,6</sup>, Jun Nyung Lee <sup>5,6</sup>, Bum Soo Kim <sup>4,5</sup>,  
Se Heang Oh <sup>1</sup> and Tae Gyun Kwon <sup>5,6</sup>

<sup>1</sup>Department of Nanobiomedical Science & BK21 PLUS NBM Global Research Center for Regenerative Medicine, Dankook University, Cheonan, Korea

<sup>2</sup>BioMedical Research Institute, Kyungpook National University Hospital, Daegu, Korea

<sup>3</sup>Joint Institution for Regenerative Medicine, Kyungpook National University Hospital, Daegu, Korea

<sup>4</sup>Department of Urology, Kyungpook National University Hospital, Daegu, Korea

<sup>5</sup>Department of Urology, School of Medicine, Kyungpook National University, Daegu, Korea

<sup>6</sup>Department of Urology, Kyungpook National University Chilgok Hospital, Daegu, Korea

## ABSTRACT




**Background:** Tissue engineering can be used for bladder augmentation. However, conventional scaffolds result in fibrosis and graft shrinkage. This study applied an alternative polycaprolactone (PCL)-based scaffold (diameter = 5 mm) with a noble gradient structure and growth factors (GFs) (epidermal growth factor, vascular endothelial growth factor, and basic fibroblast growth factor) to enhance bladder tissue regeneration in a rat model.

**Methods:** Partially excised urinary bladders of 5-week-old male Slc:SD rats were reconstructed with the scaffold (scaffold group) or the scaffold combined with GFs (GF group) and compared with sham-operated (control group) and untreated rats (partial cystectomy group). Evaluations of bladder volume, histology, immunohistochemistry (IHC), and molecular markers were performed at 4, 8, and 12 weeks after operation.

**Results:** The bladder volumes of the scaffold and GF group recovered to the normal range, and those of the GF group showed more enhanced augmentation. Histological evaluations revealed that the GF group showed more organized urothelial lining, dense extracellular matrix, frequent angiogenesis, and enhanced smooth muscle bundle regeneration than the scaffold group. IHC for  $\alpha$ -smooth muscle actin, pan-cytokeratin,  $\alpha$ -bungarotoxin, and CD8 revealed that the GF group showed high formation of smooth muscle, blood vessel, urothelium, neuromuscular junction and low immunogenicity. Concordantly, real-time polymerase chain reaction experiments revealed that the GF group showed a higher expression of transcripts associated with smooth muscle and urothelial differentiation. In a 6-month in vivo safety analysis, the GF group showed normal histology.

**Conclusion:** This study showed that a PCL scaffold with a gradient structure incorporating GFs improved bladder regeneration functionally and histologically.

**Keywords:** Bladder Regeneration; Polycaprolactone Scaffold; Gradient Structure; Growth Factors

Yun-Sok Ha <https://orcid.org/0000-0003-3732-9814>Jae-Wook Chung <https://orcid.org/0000-0002-1055-2357>Jun Nyung Lee <https://orcid.org/0000-0002-6342-9846>Bum Soo Kim <https://orcid.org/0000-0002-4873-3049>Se Heang Oh <https://orcid.org/0000-0002-4635-6809>Tae Gyun Kwon <https://orcid.org/0000-0002-4390-0952>**Funding**

This research was supported by the Basic Science Research Program through the National Research Foundation of Korea (NRF) & funded by the Korean government (MSIT) (2018R1C1B5040264; 2019R1A2C1004046; 2019R1F1A1044473; 2019R1H1A1079839; 2020R1A2B5B03002344; 2020R111A3071568).

**Disclosure**

The authors have no potential conflicts of interest to disclose.

**Author Contributions**

Conceptualization: Chun SY, Oh SH, Kwon TG;  
Data curation: Kim HY, Chun SY, Kim B, Ha YS, Kim BS; Formal analysis: Lee EH, Chung JW, Lee JN; Writing - original draft: Chun SY, Oh SH; Writing - review & editing: Oh SH, Kwon TG.

**INTRODUCTION**

The treatment of bladder cancer requires total or partial surgical removal of the bladder. Gastrointestinal tissues are the most commonly used materials for bladder augmentation following surgery. However, the use of such tissues may cause metabolic disturbances, infections, excessive mucus production, perforation, and/or bladder stone formation.<sup>1</sup> To avoid these problems, numerous natural or synthetic materials have been tested as alternative materials in the clinical and experimental fields.<sup>2,3</sup> Synthetic materials are generally preferable owing to their advantages of having an easily manipulatable structure, mechanics, duration, consistency, and biocompatibility. Among the synthetic materials that have been used for tissue engineering, polycaprolactone (PCL) has the ideal flexibility and biocompatibility for bladder augmentation, and its debris *in vivo* has little toxicity.<sup>4</sup>

In this study, a PCL-based scaffold was made with a gradient structure because stem cell migration and differentiation are governed by the physical and chemical gradients of the scaffold.<sup>5</sup> The PCL scaffold was arranged into a multilayered pattern with large surface and inner areas. Additionally, specific growth factors (GFs) were incorporated into the PCL scaffold to promote the attachment, proliferation, and differentiation of the migrated host cells. These GFs, namely vascular endothelial growth factor (VEGF), epidermal growth factor (EGF), and basic fibroblast growth factor (bFGF), were combined with the expectation that they would stimulate blood vessel formation/maturation,<sup>6</sup> neuromuscular junction regeneration,<sup>7</sup> urothelium proliferation,<sup>8</sup> and smooth muscle layer reorganization.<sup>9,10</sup> To enhance bladder regeneration, the incorporation of urothelial and/or smooth muscle cells may also be considered, but this requires an excessively laborious and expensive process<sup>9</sup> and raises many difficulties in clinical application.

We hypothesized that a PCL scaffold with a gradient structure incorporating GFs could effectively regenerate the bladder urothelium, vascular components, and smooth muscle. The regeneration of partially cystectomized bladder treated using this scaffold was compared with that of other groups that were treated without a scaffold or GFs in a rat model at the functional and histological levels.

**METHODS****Scaffold materials and manufacture**

PCL (MW, 81 kDa; Lakeshore Biomaterials, Birmingham, AL, USA) and tetraglycol (Sigma-Aldrich, St. Louis, MO, USA) were used to fabricate a membrane-type scaffold. The scaffold was manufactured by an immersion-precipitation method as described elsewhere.<sup>2</sup> In brief, PCL powder was dissolved in tetraglycol (15 wt%) at 90°C, and the hot PCL solution was poured into a mold (50 × 50 × 0.4 mm<sup>3</sup>) and then immersed in 50% ethanol solution (17°C) for 1 hour. The precipitated membrane was removed from the mold, washed with water for 6 hours, and then vacuum dried. The scaffold was trimmed into a circular shape (diameter = 5 mm and thickness around 0.4 mm).

**Morphology analysis**

With a scanning electron microscope (S-4300; Hitachi, Tokyo, Japan), the scaffold's pore size, roughness of the top and bottom surfaces, and vertical structure of a cross-section were observed.

### GFs incorporation and release behavior

For the incorporation of the GFs (EGF, VEGF, and bFGF) into the scaffold, first the EGF solution (200 ng/mL in phosphate-buffered saline [PBS] supplemented with 1% bovine serum albumin) was added to a syringe (10 mL) containing the scaffold. The EGF solution was infiltrated into the membrane under positive pressure. The membrane immersed in the EGF solution was incubated (adsorbed) at 4°C for 3 hours, rinsed with PBS, and freeze-dried. Then, bFGF and VEGF were sequentially incorporated into the EGF-loaded membrane using the same procedures as described above. The concentrations of each GF solution were selected through our preliminary studies to optimize loading amount and release behavior of each GF. For each GF, the concentration that was successfully incorporated into the scaffold was quantified by direct enzyme-linked immunosorbent assay (ELISA) using a commercial ELISA kit (DuoSet<sup>®</sup>; R&D Systems, Minneapolis, MN, USA). To investigate the release behavior of the GFs, the scaffold was incubated in 1 mL PBS supplemented with 1% bovine serum albumin at 37°C with mild shaking (50 rpm). The solution was harvested every day and replaced with the same volume of fresh PBS. The amount of each GF released was determined by ELISA as described above.

### Animal grouping and surgical procedures for in vivo study

Eighty 5-week-old male Slc:SD rats were divided into 4 groups: 1) control group, sham-operated; 2) partial cystectomy group, in which a defect of approximately 50% was created in the dome of the bladder wall; 3) scaffold group, the scaffold without GFs was attached after partial cystectomy; and 4) GF group, the scaffold with incorporated GFs was attached after partial cystectomy. Animals were anesthetized with 16 mg/kg of rompun and 0.04 mg/kg zoletil by intramuscular injection. After abdominal incision, the bladder was exposed and a partial cystectomy was made. The scaffold was sutured as a patch onto the defect of the bladder with 7-0 Vicryl<sup>™</sup> sutures. The rough surface of the scaffold was located on the inner wall of the bladder. The abdominal wound was closed, and 15 mg/kg of cefprozil was administered with intramuscular injection to prevent procedure-related infections. The animals were observed in warm cages until they woke up completely. All of the procedure was carried by a urologic specialist. Animals were sacrificed 4, 8, and 12 weeks after surgery (each group, n = 5). A separate set of GF group animals were maintained for 6 months to survey the long-term in vivo safety of the scaffold (n = 3).

### Bladder volume measurements

Measurements of bladder volume were performed at each time point in each group. After anesthesia, a catheter was inserted directly into the bladder surgically. The bladder was continuously filled with distilled water (150  $\mu$ L/min) via a syringe pump using the PowerLab<sup>®</sup> system (ADInstruments, Dunedin, New Zealand), and the maximal volume was calculated as the total amount of water input at the time of the first urine leakage. The measurement was repeated at least three times. Finally, the entire bladder was removed and divided into two portions for use in histology and molecular analyses.

### Evaluations of histology, immunohistochemistry (IHC), gene expression, and in vivo safety

Half of each bladder was fixed in formalin, embedded in paraffin, cut into 5- $\mu$ m sections, and then subjected to hematoxylin and eosin (H&E) staining or IHC. The histopathological analyses were performed by an experienced pathologist. The regenerated smooth muscle bundle, urothelium layers, and neuromuscular junctions were identified by IHC with antibodies against  $\alpha$ -smooth muscle actin ( $\alpha$ -SMA), pan-cytokeratin, and  $\alpha$ -bungarotoxin

( $\alpha$ -BUN), respectively. All these antibodies were used at 1:100 dilution and were purchased from Sigma-Aldrich. Angiogenesis was measured by counting blood vessels that were positively stained for H&E and  $\alpha$ -SMA in the scaffold implant area. Five different sites were observed at 200  $\times$  magnification. Immune cell infiltrates were identified using a T-lymphocyte-specific antibody (CD8, 1:100; Sigma-Aldrich). The tissue samples were incubated with the primary antibody overnight at 4°C followed by incubation with an appropriate secondary antibody for 1 hour (Alexa Fluor® 594; Life Technologies, Waltham, MA, USA), and nuclei were stained with 4',6-diamidino-2-phenylindole.

The regeneration of smooth muscle and urothelium was confirmed by measuring the expression of differentiation-related genes using real-time polymerase chain reaction (PCR). RNA was extracted with TRIzol® reagent, and cDNA synthesis was performed with 20  $\mu$ g of total RNA using the SuperScript® Choice cDNA synthesis kit with SYBR® Green (Thermo Fisher Scientific, Waltham, MA, USA). The PCR conditions were 95°C for 10 minutes, followed by 40 cycles of 95°C for 10 seconds, 58°C for 50 seconds, and 72°C for 20 seconds. To analyze the relative changes in gene expression, the 2<sup>- $\Delta\Delta$ Ct</sup> method was used. The primer sequences are shown in Table 1.

### Statistical analysis

The data were presented as the mean  $\pm$  standard deviation. Differences among groups in the results of the bladder volume and real-time PCR evaluations were analyzed by one-way analysis of variance. A *P* value of < 0.05 was considered to indicate statistical significance. If significant differences were identified by the analysis of variance, then Tukey's post hoc test was conducted.

**Table 1.** Gene information for real-time polymerase chain reaction

Categories	Gene product	Full name	Primer sequences
Smooth muscle differentiation	MyoD	Myoblast determination protein	5'-ACAGCGCGTTTTTCCAC 5'-AACCTAGCCCTCAAGGTTTCAG
	Desmin	Desmin	5'-GGAGAGGAGAGCCGGATCA 5'-GGGCTGGTTTCTCGGAAGTT
	Myosin	Myosin	5'-AGGCGGAGAGGTTTTCCAA 5'-CTTGTAGTCCAAGTTGCCAGTCA
	$\alpha$ -SMA	Alpha smooth muscle actin	5'-CAAGTGATCACCATCGGAAATG 5'-GACTCCATCCCGATGAAGGA
	Urothelium differentiation	UP1a	Uroplakin 1A
UP1b		Uroplakin 1B	5'-CAATTGCTGTGGCGTAAATGG 5'-ATAACACAGCATTGACGAGGCC
UP2		Uroplakin 2	5'-TCGTGCCAGGAACCAAATTC 5'-GGATTCCATGTTCTTCGAGG
CK7		Cytokeratin-7	5'-GGAATCATGAGCGTGAAGCT 5'-CCAGTGAATTCATCACAGAGA
CK13		Cytokeratin-13	5'-GGATGCTGAGGAATGGTTCCA 5'-GCTCTGTCTTGCTCCGTGATCT
CK18		Cytokeratin-18	5'-ATTGAGGAGAGCACACAGTGG 5'-TTCATGGAGTCCAGGTCGATC
CK19		Cytokeratin-19	5'-CAGGTCAGTGTGGAGGTGGAT 5'-TCGCATGTCCTCAGGATCTTG
PAN-CK		Pan-cytokeratin	5'-GCCTCCTTGGCAGAAACAGAA 5'-GCACTCGGTTTCAGCTCGAAT
GAPDH		Glyceraldehyde-3-phosphate dehydrogenase	5'-TGTGTCCGTCGTGGATCTGA 5'-CCTGCTTACCACCTTCTTGA

**Ethics statement**

This study was approved by the Ethics Committee on Animal Research of Kyungpook National University, College of Medicine (KNUCH 2018-08-008-003).

**RESULTS**

**Scaffold morphology**

The top and bottom surfaces and cross-sectional morphologies of the scaffold were imaged by scanning electron microscopy (Fig. 1A). The scaffold had a smooth top surface (Fig. 1A) with nano-sized pores (around 100 nm) and a rough bottom surface (Fig. 1A) with micro-sized pores (around 100 μm). The cross-section (Fig. 1A) showed a gradient pore size along the vertical orientation with a looser structure towards the upward direction and a denser structure towards the downward direction.

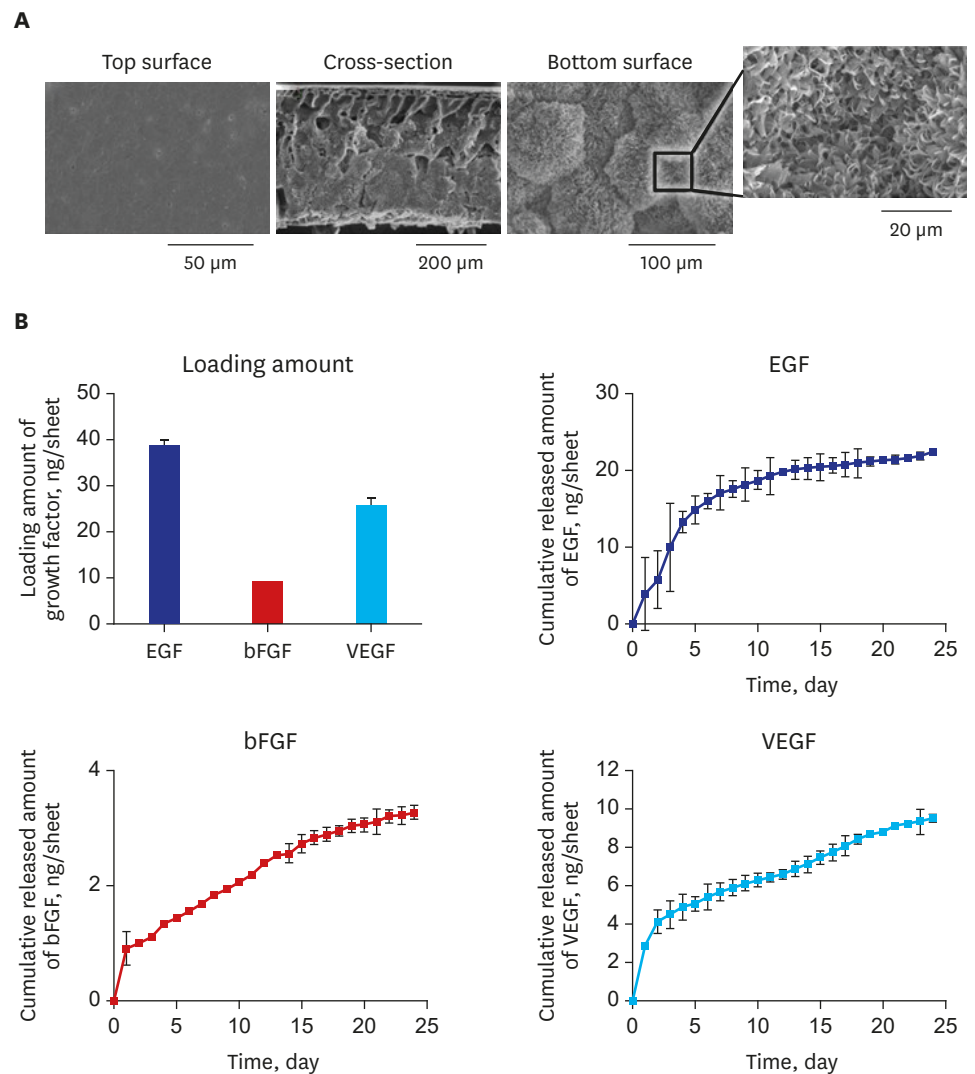


**Fig. 1.** Polycaprolactone-based scaffold with a gradient structure and incorporated growth factors. (A) Scanning electron microscopy photographs of the top/bottom surfaces and the cross-sectional morphology. (B) Loading amount of each growth factor (ng/sheet) and sustained release of the growth factors from the scaffold for 25 days. EGF = epidermal growth factor, VEGF = vascular endothelial growth factor, bFGF = basic fibroblast growth factor.

### Loading amount and release behavior of GFs in vitro

The loading amounts of EGF, bFGF, and VEGF immobilized into the scaffold were  $38.98 \pm 1.60$ ,  $9.02 \pm 0.23$ , and  $25.53 \pm 1.84$  ng/sheet, respectively (Fig. 1B). The most abundant GF in the scaffold was EGF, followed by VEGF and bFGF. The different loading amount of GFs can be understood by electrostatic interactions among the GFs during their sequential loading procedures. The VEGF (isoelectric point [pI], around 9.6; positively charged in PBS) can form attractive interactions with EGF (pI, around 5.53; negatively charged in PBS) immobilized on the pore surfaces of scaffold, but the bFGF (pI, around 8.5; positively charged in PBS) can form both attractive and repulsive interactions with EGF and VEGF immobilized on the pore surfaces of scaffold. The kinetics of the release of GFs from the scaffold are shown in Fig. 1B. All the GFs were continuously released without any remarkable initial burst for 24 days, at which point the amounts released relative to the amounts loaded were around 56% (EGF), around 36% (bFGF), and around 37% (VEGF). The release of the GFs continued after the 24th day.

### Animal survival rate and bladder gross images in vivo

All the rats survived until their scheduled sampling, and there were no significant changes in body weight, incontinence, urinary tract infection, diverticulum, leakage, or voiding problems (data not shown). For 12 weeks, scaffold remnants were visible at the site of implantation in both the scaffold and GF groups (Fig. 2A, arrow). The scaffold gradually shrank to two-thirds of its initial size at week 12, and the top surface of each scaffold was covered with a fibrotic membrane. The partial cystectomy group showed scar tissue formation in the dome area. The bladders of the scaffold and GF groups were restored to almost their original volumes at week 12 (Fig. 2A), but those of the partial cystectomy group remained at about half of their original volumes. Thirty percent of rats in both the scaffold and GF groups showed bladder stone formation, and the sizes of the stones varied (data not shown).

### Bladder volume measurements

The bladder volume was calculated as the amount of distilled water input at the time of first leakage (Fig. 2B). At weeks 4, 8, and 12, the bladder volumes of the GF group were  $1,330 \pm 147$ ,  $1,700 \pm 312$ , and  $1,650 \pm 300$   $\mu$ L, those of the scaffold group were  $907.5 \pm 143$ ,  $1,245 \pm 150$ , and  $1,291 \pm 443$   $\mu$ L, and those of the partial cystectomy group were  $270 \pm 106$ ,  $372.5 \pm 31$ , and  $573 \pm 111$   $\mu$ L, respectively. This result means that bladder augmentation was achieved through the attachment of the scaffold, and the GF group showed a significantly greater increase in bladder volume than the scaffold group ( $P < 0.05$ ).

### Histological, IHC, and gene expression evaluations

The results of histology with H&E staining (Fig. 2C) showed that the scaffold was maintained for 12 weeks. With the scaffold, regenerated urothelial layers, connective tissues, blood vessels, and smooth muscle bundles appeared. At week 12, the urothelial layer was regenerated in both the experimental groups, but the GF group showed a more organized multilayer structure of the regenerated urothelium, with a distinct basal layer and umbrella cells (arrow). The regeneration of the urothelium progressed faster than that of the muscle layer. Regenerated smooth muscle bundles appeared at week 12, and the GF group showed thicker and denser bundles than the scaffold group. The submucosal tissue was composed of connective tissue and blood vessels. The GF group showed a tighter connective tissue layer and a more frequent appearance of blood vessels than the scaffold group. Infiltrated inflammatory cells were found under the urothelium, mainly consisting of granulocytes in addition to some lymphocytes and macrophages. The frequency at which inflammatory cells appeared was higher in the scaffold group than in the GF group and reduced over time in both groups.



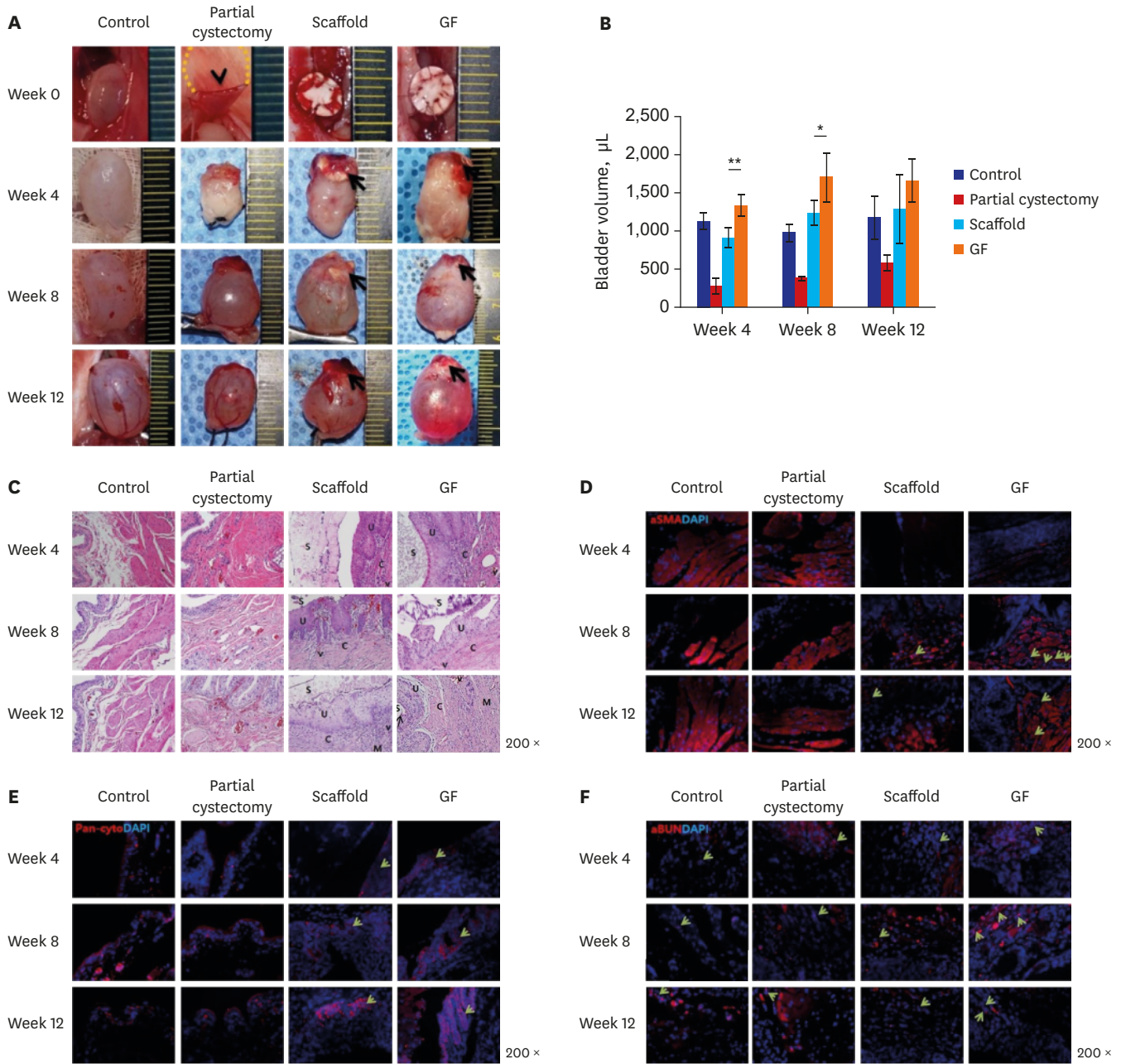


**Fig. 2.** In vivo analysis of morphological and histological aspects. **(A)** Gross images. The partial cystectomy (arrowhead), scaffold remnants (arrow), tightly sutured scaffold on the bladder at week 0, and restored bladder volume at week 12 are indicated. **(B)** Bladder volume measurements at weeks 4, 8, and 12 after the cystectomy operation. **(C)** Histological analysis with hematoxylin and eosin staining. Regenerated urothelial layers (U), connective tissues (C), blood vessels (V), smooth muscle bundles (M) and scaffold (S) were marked. **(D-G)** Immunohistochemistry with antibodies specific to  $\alpha$ -smooth muscle actin to detect the smooth muscle bundle and blood vessels (**D**, arrows indicate newly-formed blood vessels); pan-cytokeratin to detect the urothelium (**E**, arrows indicate newly-formed urothelium at the border of the regenerated tissue);  $\alpha$ -bungarotoxin to detect neuromuscular junctions (**F**, arrows indicate newly-formed neuromuscular junctions in the smooth muscle bundle); and CD8 to detect cytotoxic T cells (**G**, arrows indicate positively stained cells and the size of each arrow corresponds to the distribution of the cells). Control = sham-operated group, Partial cystectomy = the group with a 50% defect created by surgery, Scaffold = the group treated using the unmodified scaffold after partial cystectomy, GF = the group treated using the scaffold with incorporated growth factors (epidermal growth factor, vascular endothelial growth factor, and basic fibroblast growth factor) after partial cystectomy. \* $P < 0.05$ ; \*\* $P < 0.01$ .

(continued to the next page)

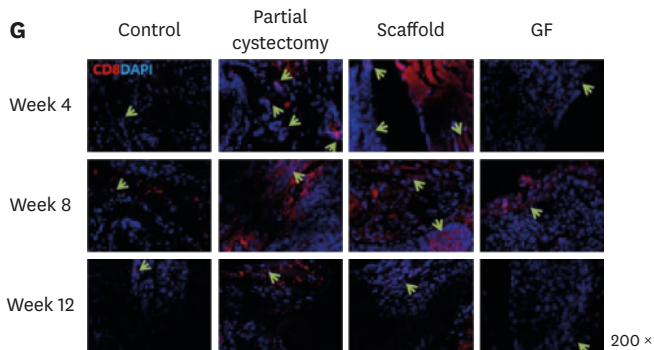


**Fig. 2.** (Continued) In vivo analysis of morphological and histological aspects. **(A)** Gross images. The partial cystectomy (arrowhead), scaffold remnants (arrow), tightly sutured scaffold on the bladder at week 0, and restored bladder volume at week 12 are indicated. **(B)** Bladder volume measurements at weeks 4, 8, and 12 after the cystectomy operation. **(C)** Histological analysis with hematoxylin and eosin staining. Regenerated urothelial layers (U), connective tissues (C), blood vessels (V), smooth muscle bundles (M) and scaffold (S) were marked. **(D-G)** Immunohistochemistry with antibodies specific to  $\alpha$ -smooth muscle actin to detect the smooth muscle bundle and blood vessels (**D**, arrows indicate newly-formed blood vessels); pan-cytokeratin to detect the urothelium (**E**, arrows indicate newly-formed urothelium at the border of the regenerated tissue);  $\alpha$ -bungarotoxin to detect neuromuscular junctions (**F**, arrows indicate newly-formed neuromuscular junctions in the smooth muscle bundle); and CD8 to detect cytotoxic T cells (**G**, arrows indicate positively stained cells and the size of each arrow corresponds to the distribution of the cells). Control = sham-operated group, Partial cystectomy = the group with a 50% defect created by surgery, Scaffold = the group treated using the unmodified scaffold after partial cystectomy, GF = the group treated using the scaffold with incorporated growth factors (epidermal growth factor, vascular endothelial growth factor, and basic fibroblast growth factor) after partial cystectomy. \* $P < 0.05$ ; \*\* $P < 0.01$ .

Smooth muscle, blood vessels, urothelial layers, and neuromuscular junctions were recognized with IHC staining using antibodies against  $\alpha$ -SMA, pan-cytokeratin, and  $\alpha$ -BUN, respectively (**Fig. 2D-F**). The smooth muscle bundle was visible throughout the entire regenerated area and was much more pronounced in the GF group than in the scaffold group (**Fig. 2D**). The  $\alpha$ -SMA antibody also revealed mature blood vessels (**Fig. 2D**, arrow), since they included a component of smooth muscle. The number of regenerated blood vessels in the GF group was significantly higher ( $3.14 \pm 0.01$ ) than that in the scaffold group ( $1.05 \pm 0.02$ ) ( $P < 0.01$ ) and was similar to that in the sham-operated group ( $3.52 \pm 0.13$ ). The urothelial layers of the GF group were more organized than those in the scaffold group (**Fig. 2E**). The frequency of neuromuscular junctions in the GF group was higher than that in the scaffold group (**Fig. 2F**). To analyze the in vivo immune reaction to the scaffold, a CD8 antibody was used to detect infiltrated T-lymphocytes (**Fig. 2G**). The scaffold group showed the presence of T-lymphocytes in the urothelial and smooth muscle layers at week 8, while the GF group showed positivity only in one region of the urothelial layer. At week 12, the scaffold group showed weak positive staining for CD8 in the connective tissue area, while no staining could be detected in the GF group.

For the molecular evaluation of the regenerated smooth muscle and urothelial layers, the expression of differentiation-related genes was analyzed (**Fig. 3A and B**). The expression of the genes encoding MyoD, desmin, myosin, and  $\alpha$ -SMA, which have been widely used as markers of smooth muscle differentiation, was significantly higher in the GF group than in the scaffold group ( $P < 0.05$ ) (**Fig. 3A**). Similarly, the expression of the genes encoding UP-1a, -1b, and -2, CK-13, -18, and -19, and pan-cytokeratin, which have been widely used as markers of squamous differentiation in the urothelium, was also significantly higher in the GF group than in the scaffold group ( $P < 0.05$ ) (**Fig. 3B**).

In our long-term (6-month) in vivo safety test of the GF group, histological evaluations displayed no abnormality, toxicity, or inflammatory response in the regenerated tissues after 6 months (**Fig. 4**).



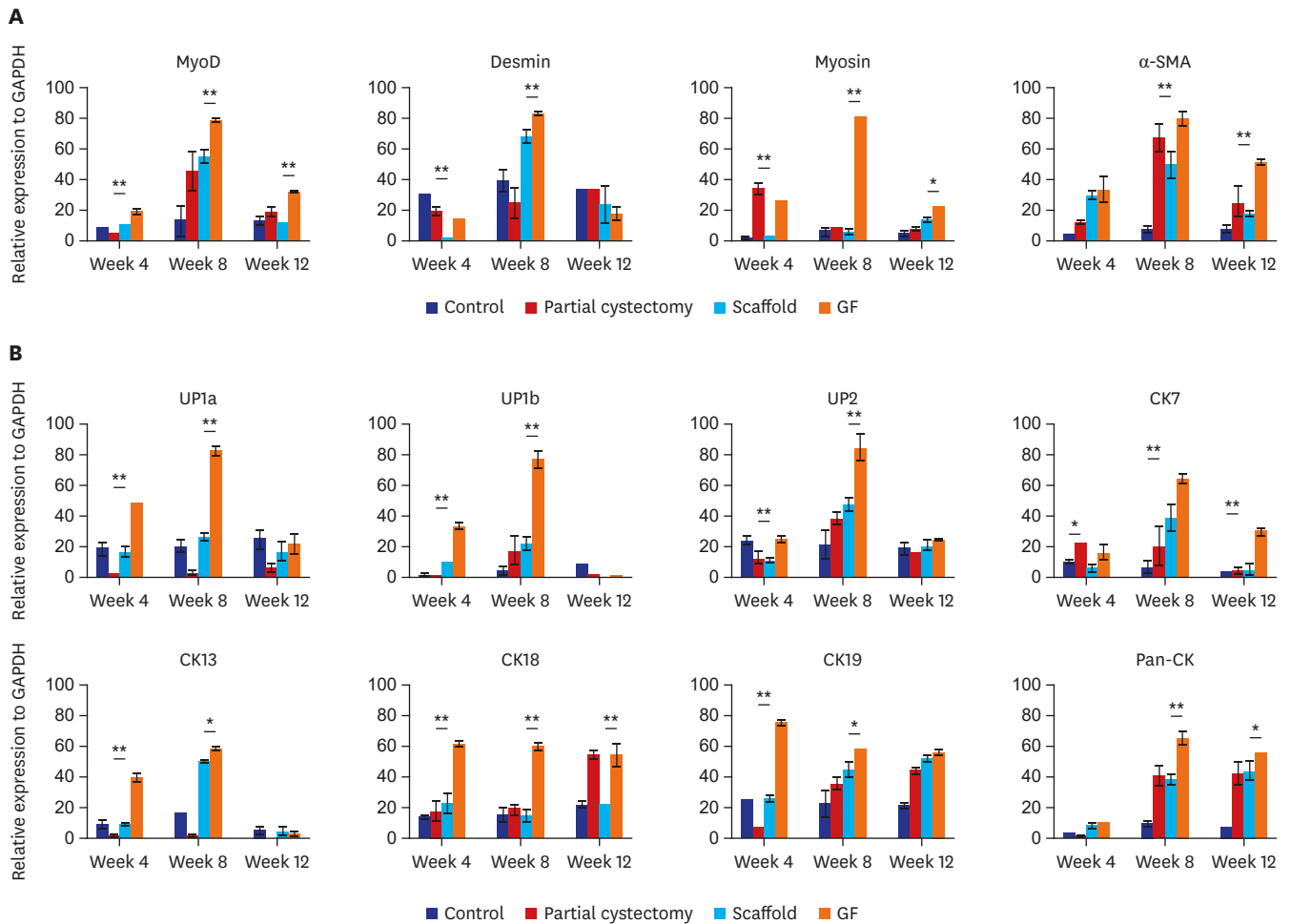


**Fig. 3.** In vivo analysis of gene expression. The smooth muscle (A) and urothelium (B) differentiation related gene expression. Control = sham-operated group, Partial cystectomy = the group with a 50% defect created by surgery, Scaffold = the group treated using the unmodified scaffold after partial cystectomy, GF = the group treated using the scaffold with incorporated growth factors (epidermal growth factor, vascular endothelial growth factor, and basic fibroblast growth factor) after partial cystectomy. MyoD = Myoblast determination protein,  $\alpha$ -SMA = alpha smooth muscle actin, UP1a = uroplakin 1A, UP1b = uroplakin 1B, UP2 = uroplakin 2, CK7 = cytokeratin-7, CK13 = cytokeratin-13, CK18 = cytokeratin-18, CK19 = cytokeratin-19, PAN-CK = pan-cytokeratin, GAPDH = glyceraldehyde-3-phosphate dehydrogenase. \* $P < 0.05$ ; \*\* $P < 0.01$ .

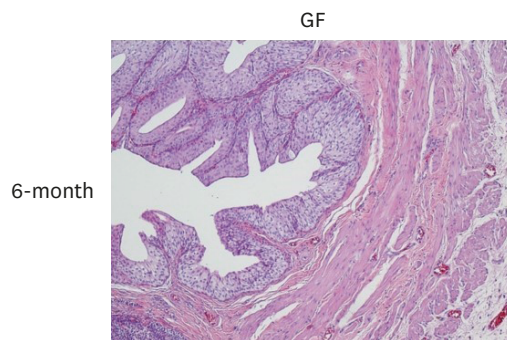


**Fig. 4.** In vivo 6-month safety. GF = the group treated using the scaffold with incorporated GFs (epidermal growth factor, vascular endothelial growth factor, and basic fibroblast growth factor) after partial cystectomy.

## DISCUSSION

In the present study, we manufactured a scaffold with a gradient structure and different roughnesses on its top and bottom sides for bladder regeneration. The gradient structure was formed by immersing the scaffold into a 50% ethanol solution at a low temperature.<sup>5</sup> The solubility of PCL decreases when the temperature of the immersion solution is low or mixed with alcohol, which causes a gradual accumulation of the precipitate.<sup>6</sup> The gradient structure could stimulate cell differentiation, because spatial differences in the density of adhered cells promote cell differentiation<sup>11</sup> and this structure provided a large surface area for host cell migration, adhesion, and proliferation.<sup>12</sup> A smooth surface with small pores prevents the adhesion and infiltration of fibrotic cells, while a rough surface stimulates the migration and adhesion of precursor cells from the surrounding bladder tissue.<sup>13,14</sup> Furthermore, this scaffold enabled a sustained release of the incorporated GFs without the use of chemical cross-linking agents for immobilization, since its labyrinthine three-dimensional structure provided a complex path and thus the GFs incorporated into the scaffold were gradually released over an extended period.

The scaffold with these advantages was evaluated for its efficacy in facilitating bladder tissue regeneration through an *in vivo* study. There were no premature deaths among the animals during the experiment, which suggests that the surgical procedure and scaffold biocompatibility were appropriate. In previous studies, when the scaffold was attached loosely to the bladder, urine leaked into the abdominal cavity, resulting in the death of the experimental rats. In the present study, the diameter of the scaffold was 5 mm. While it may be preferable to use a larger scaffold for assessing bladder regeneration *in vivo*, the size was limited by the rat model. For 12 weeks, remnant scaffold was visible at the implantation site, and the size of the scaffold gradually reduced to reach two-thirds of its original size at 12 weeks. The low degradation rate of the scaffold is thought to have supported the ingrowth of endogenous cells,<sup>15</sup> the slow production of debris likely resulted in less inflammatory/fibrotic responses,<sup>16</sup> and muscle regeneration requires an extended period of time.<sup>17</sup> Thus, the scaffold prepared this time has a suitable degradation rate for migration of cells required for bladder regeneration.

Next, the effect of incorporating GFs into the scaffold with the intention of further promoting bladder tissue regeneration was analyzed. The bladder volume was significantly increased in the GF group as compared with the group treated with the scaffold without GFs. The histological analyses showed that blood vessel formation and maturation were increased in the GF group, which is thought to be attributable to the actions of VEGF and EGF.<sup>6</sup> This improved angiogenesis likely contributed to the enhanced regeneration of the urothelial layer and smooth muscle bundle. Additionally, urothelial cell proliferation and smooth muscle ingrowth would likely have been directly influenced by bFGF and EGF.<sup>18-20</sup> Histological regeneration of the bladder is typically associated with the expression of differentiation-related genes. Concordantly, the expression of genes encoding smooth muscle differentiation markers (MyoD, desmin, myosin, and  $\alpha$ -SMA) and squamous urothelium differentiation markers (UP-1a, -1b, and -2, CK-13, -18, and -19, and pan-cytokeratin) was significantly higher in the GF group than in the scaffold group. This finding implies that the incorporated GFs stimulated the differentiation of host stem cells into smooth muscle and urothelium through a paracrine effect, since the implanted scaffold did not initially contain any cells. Additionally, the implantation of the scaffold with incorporated GFs induced an increase in the amount of positive immunostaining for  $\alpha$ -BUN. For the muscles to work and

maintain homeostasis, they need to have an interface (termed a neuromuscular junction) with a neuron. The nerve secretes acetylcholine, which acts through receptors on the neuromuscular junction, and to detect the presence of neuromuscular junctions,  $\alpha$ -BUN is used as an acetylcholine antagonist.<sup>21</sup> The GF group showed a significant increase in positive staining for  $\alpha$ -BUN, which is thought to be attributable to the actions of VEGF and bFGF incorporated into the scaffold.<sup>22,23</sup>

Synthetic biomaterials are considered to be less immunogenic than natural matrix components, because synthetic polymers do not contain allogeneic or xenogeneic antigens. In addition, the debris from synthetic biomaterials is typically excreted and does not cause an acute or chronic immune response.<sup>24</sup> However, adverse reactions from the host could occur depending on the manufacturing process, degradation rate, or incorporated GFs; thus, we investigated the in vivo immune response of the host against the scaffold using an anti-CD8 antibody. The group implanted with the scaffold without GFs showed a similar degree of inflammation as the partial cystectomy group, while the GF group showed a lower immune response. Thus, the PCL scaffold with incorporated GFs can apparently promote bladder regeneration without the induction of problematic immune responses. Finally, the scaffold with incorporated GFs needed to be evaluated for its long-term in vivo safety, because not only the polymer itself but also the incorporated GFs may cause abnormal proliferation.<sup>25</sup> Our findings showed that the scaffold with incorporated GFs showed no tendency to cause abnormal proliferation or cancer formation.

This study demonstrated that a synthetic scaffold with a gradient structure and incorporated growth factors showed a controlled release of the GFs, retained its biological activity, and exhibited good long-term in vivo safety in a partial cystectomy rat model. Thus, this scaffold shows the potential to be developed as a clinical treatment for enhancing bladder tissue regeneration following surgery.

## REFERENCES

1. Mills RD, Studer UE. Metabolic consequences of continent urinary diversion. *J Urol* 1999;161(4):1057-66.  
[PUBMED](#) | [CROSSREF](#)
2. Atala A, Bauer SB, Soker S, Yoo JJ, Retik AB. Tissue-engineered autologous bladders for patients needing cystoplasty. *Lancet* 2006;367(9518):1241-6.  
[PUBMED](#) | [CROSSREF](#)
3. Zhao Y, He Y, Guo JH, Wu JS, Zhou Z, Zhang M, et al. Time-dependent bladder tissue regeneration using bilayer bladder acellular matrix graft-silk fibroin scaffolds in a rat bladder augmentation model. *Acta Biomater* 2015;23:91-102.  
[PUBMED](#) | [CROSSREF](#)
4. Lee JN, Chun SY, Lee HJ, Jang YJ, Choi SH, Kim DH, et al. Human urine-derived stem cells seeded surface modified composite scaffold grafts for bladder reconstruction in a rat model. *J Korean Med Sci* 2015;30(12):1754-63.  
[PUBMED](#) | [CROSSREF](#)
5. Di Luca A, Szlczak K, Lorenzo-Moldero I, Ghebes CA, Lepedda A, Swieszkowski W, et al. Influencing chondrogenic differentiation of human mesenchymal stromal cells in scaffolds displaying a structural gradient in pore size. *Acta Biomater* 2016;36:210-9.  
[PUBMED](#) | [CROSSREF](#)
6. Nillesen ST, Geutjes PJ, Wismans R, Schalkwijk J, Daamen WF, van Kuppevelt TH. Increased angiogenesis and blood vessel maturation in acellular collagen-heparin scaffolds containing both FGF2 and VEGF. *Biomaterials* 2007;28(6):1123-31.  
[PUBMED](#) | [CROSSREF](#)

7. Lee SH, Jin WP, Seo NR, Pang KM, Kim B, Kim SM, et al. Recombinant human fibroblast growth factor-2 promotes nerve regeneration and functional recovery after mental nerve crush injury. *Neural Regen Res* 2017;12(4):629-36.  
[PUBMED](#) | [CROSSREF](#)
8. Freeman MR, Yoo JJ, Raab G, Soker S, Adam RM, Schneck FX, et al. Heparin-binding EGF-like growth factor is an autocrine growth factor for human urothelial cells and is synthesized by epithelial and smooth muscle cells in the human bladder. *J Clin Invest* 1997;99(5):1028-36.  
[PUBMED](#) | [CROSSREF](#)
9. Roelofs LA, Kortmann BB, Oosterwijk E, Eggink AJ, Tiemessen DM, Crevels AJ, et al. Tissue engineering of diseased bladder using a collagen scaffold in a bladder exstrophy model. *BJU Int* 2014;114(3):447-57.  
[PUBMED](#)
10. Kanematsu A, Yamamoto S, Noguchi T, Ozeki M, Tabata Y, Ogawa O. Bladder regeneration by bladder acellular matrix combined with sustained release of exogenous growth factor. *J Urol* 2003;170(4 Pt 2):1633-8.  
[PUBMED](#) | [CROSSREF](#)
11. Di Luca A, Ostrowska B, Lorenzo-Moldero I, Lepedda A, Swieszkowski W, Van Blitterswijk C, et al. Gradients in pore size enhance the osteogenic differentiation of human mesenchymal stromal cells in three-dimensional scaffolds. *Sci Rep* 2016;6:22898.  
[PUBMED](#) | [CROSSREF](#)
12. Kellomäki M, Niiranen H, Puumanen K, Ashammakhi N, Waris T, Törmälä P. Bioabsorbable scaffolds for guided bone regeneration and generation. *Biomaterials* 2000;21(24):2495-505.  
[PUBMED](#) | [CROSSREF](#)
13. Guarino V, Ambrosio L. *Electrofluidodynamic Technologies (EFDTs) for Biomaterials and Medical Devices: Principles and Advances*. Duxford: Woodhead Publishing; 2018.
14. Deng Y, Kuiper J. *Functional 3D Tissue Engineering Scaffolds: Materials, Technologies, and Applications*. Duxford: Woodhead Publishing; 2017.
15. Chen W, Shi C, Hou X, Zhang W, Li L. Bladder acellular matrix conjugated with basic fibroblast growth factor for bladder regeneration. *Tissue Eng Part A* 2014;20(15-16):2234-42.  
[PUBMED](#) | [CROSSREF](#)
16. Khang G. *Handbook of Intelligent Scaffolds for Tissue Engineering and Regenerative Medicine*. Singapore: Pan Stanford Publishing; 2017.
17. Wefer J, Sievert KD, Schlote N, Wefer AE, Nunes L, Dahiya R, et al. Time dependent smooth muscle regeneration and maturation in a bladder acellular matrix graft: histological studies and in vivo functional evaluation. *J Urol* 2001;165(5):1755-9.  
[PUBMED](#) | [CROSSREF](#)
18. Beqaj SH, Donovan JL, Liu DB, Harrington DA, Alpert SA, Cheng EY. Role of basic fibroblast growth factor in the neuropathic bladder phenotype. *J Urol* 2005;174(4 Pt 2):1699-703.  
[PUBMED](#) | [CROSSREF](#)
19. Imamura M, Kanematsu A, Yamamoto S, Kimura Y, Kanatani I, Ito N, et al. Basic fibroblast growth factor modulates proliferation and collagen expression in urinary bladder smooth muscle cells. *Am J Physiol Renal Physiol* 2007;293(4):F1007-17.  
[PUBMED](#) | [CROSSREF](#)
20. Borer JG, Park JM, Atala A, Nguyen HT, Adam RM, Retik AB, et al. Heparin-binding EGF-like growth factor expression increases selectively in bladder smooth muscle in response to lower urinary tract obstruction. *Lab Invest* 1999;79(11):1335-45.  
[PUBMED](#)
21. Young HS, Herbette LG, Skita V.  $\alpha$ -bungarotoxin binding to acetylcholine receptor membranes studied by low angle X-ray diffraction. *Biophys J* 2003;85(2):943-53.  
[PUBMED](#) | [CROSSREF](#)
22. Zheng C, Sköld MK, Li J, Nennesmo I, Fadeel B, Henter JI. VEGF reduces astrogliosis and preserves neuromuscular junctions in ALS transgenic mice. *Biochem Biophys Res Commun* 2007;363(4):989-93.  
[PUBMED](#) | [CROSSREF](#)
23. Chen C. *Presynaptic Differentiation at the Neuromuscular Junction: Regulation by a Novel bFGF-p120 Catenin Signaling Pathway [dissertation]*. Hong Kong: Hong Kong University of Science and Technology; 2007.
24. Vishwakarma A, Sharpe P, Shi S, Ramalingam M. *Stem Cell Biology and Tissue Engineering in Dental Sciences*. Amsterdam: Academic Press; 2014.
25. Goustin AS, Leof EB, Shipley GD, Moses HL. Growth factors and cancer. *Cancer Res* 1986;46(3):1015-29.  
[PUBMED](#)